

# Map-based molecular diversity, linkage disequilibrium and association mapping of fruit traits in melon

Yan Tomason · Padma Nimmakayala ·  
Amnon Levi · Umesh K. Reddy

Received: 9 October 2012 / Accepted: 17 January 2013 / Published online: 2 February 2013  
© Springer Science+Business Media Dordrecht 2013

**Abstract** Melon has tremendous fruit diversity, the product of complex interactions of consumer preferences in different countries and a wide range of agro-climatic zones. Understanding footprints of divergence underlying formation of various morphotypes is important for developing sustainable and high-quality melons. Basic understanding of population structure and linkage disequilibrium (LD) is limited in melon and has lagged behind other crops. Characterization of population structure and LD are essential for carrying out association mapping of quantitative trait loci (QTL) underlying various complex traits. Mapped single-locus microsatellite markers are known to be very valuable for resolving the population structure

and 268 such markers were used in the current study to resolve population structure and LD pattern using 87 accessions of melons belonging to Eastern European, Euro-North American and Asian types. A mixed linear model was implemented to detect QTL for various fruit traits. Various levels of QTL with high to moderate stringency were detected for fruit shape, fruit weight, soluble solids, and rind pressure and a majority of them was found to be in agreement with the previously published data, indicating that association mapping can be very useful for melon molecular breeding. Minor discrepancies in the position, strength and the variation explained by the QTL present between the methods of association and recombinant mapping approaches can be bridged if more melon groups and larger sets of accessions are involved in future studies, combined with high-throughput marker panels.

---

Padma Nimmakayala: Contributed equally to the first author.

**Electronic supplementary material** The online version of this article (doi:10.1007/s11032-013-9837-9) contains supplementary material, which is available to authorized users.

---

Y. Tomason · P. Nimmakayala · U. K. Reddy (✉)  
Department of Biology, Gus R. Douglass Institute, West  
Virginia State University, Institute, WV 25112-1000,  
USA  
e-mail: uredy@wvstateu.edu

Y. Tomason  
Dnipropetrovsk State Agrarian University,  
Dnipropetrovsk 49600, Ukraine

A. Levi  
U.S. Vegetable Laboratory, USDA, ARS, 2875 Savannah  
Highway, Charleston, SC 29414, USA

**Keywords** Linkage disequilibrium · Fruit traits ·  
Microsatellites · Melon · Population structure

## Introduction

Melon (*Cucumis melo* L.) is an economically important horticultural crop and is a diploid ( $n = 12$ ) with a genome size of 450 Mb (Arumuganathan and Earle 1991). Melons belonging to the two subspecies *melo* and *agrestis* were previously grouped under seven morphotypes: cantaloupes, honeydew, Casaba, Persian, Santa Claus, Crenshaw and Juan Canari (Munger

and Robinson 1991; Robinson and Decker-Walters 1997). According to the morphological observations of Jeffrey (1980) and Stepansky et al. (1999) vars. *cantalupensis* (cantaloupe) and *inodorus* (honeydew) should be placed in subspecies *melo* and vars. *momordica*, *conomon*, *dudaim*, and *chito* in subspecies *agrestis* (Decker-Walters et al. 2002). Pitrat (2008) grouped melons into 15 morphotypes (*cantalupensis*, *reticulatus*, *adana*, *chandalak*, *ameri*, *inodorus*, *chate*, *flexuosus*, *dudaim* and *tibish* (in subsp. *melo*), and *momordica*, *conomon*, *chinensis*, *makuwa*, and *acidulous* in subsp. *agrestis*). Many of the taxonomic groups are widely disputed as their accessions share genealogies of both *melo* and *agrestis* and are heterogenous, exhibiting mixed features (Blanca et al. 2012). However, molecular studies strongly supported the sub-specific division (Deleu et al. 2009; Stepansky et al. 1999) and Blanca et al. (2012) suggested reclassifying some of the morphotypes back to their respective subgroups based on molecular genetic relationships.

There is little information about melon germplasm from eastern Europe, particularly on how it is related to melons from Asia and the western hemisphere. Eastern European melons have a known cultivated history of about 2,500 years, as excavations from Chersonese, located on the outskirts of Sevastopol on the Crimean peninsula of Ukraine, have unearthed fossilized melon seeds (Pangalo 1958). Melons are known to have been cultivated in the territory of Ukraine and Russia for about 25 centuries, and the genealogy records of these melon types have been traced to eastern and central Asian lineages (Pyzhenkov and Malinina 1994). Currently the particular market group of melons that are broadly known as *adana* occupy about 50 thousand hectares throughout eastern Europe (Nimmakayala et al. 2009). Based on genome-wide transcript-based SNP profiles, eastern European germplasm was considered as basal to the taxonomic group of *cantalupensis* (Blanca et al. 2012).

Current research has been designed to take advantage of the abundance of melon genetic diversity to perform association mapping (syn. linkage disequilibrium mapping) to resolve complex trait variation and identify quantitative trait loci (QTL). This approach offers three advantages over traditional linkage analysis: (1) increased mapping resolution; (2) increased efficiency (reduced resources), and (3) the ability to identify diverse alleles (Yu and Buckler

2006; Risch and Merikangas 1996; Nordborg and Tavare 2002). Association mapping has been widely used in all the major crops including maize, rice, barley, tomato, wheat, sorghum, sugarcane, soybean, grape and several tree and grass species (Zhang et al. 2011). It has proved to be very effective for mining new genes if the population structure can be resolved accurately to reduce spurious associations due to confounding effects of subpopulations. For estimating population structure ( $Q$ ) and relative kinship matrix ( $K$ ), the multi-allelic and codominant microsatellites can be very useful as they are selectively neutral (Zhu et al. 2008) and recent when compared to single nucleotide polymorphisms (SNPs) (Remington et al. 2001). A unified mixed model approach for association mapping in combination with  $Q$  and  $K$  provides a dependable and robust system for identification of reliable QTL (Zhao et al. 2007). Most ideal background markers that are required to accurately estimate  $Q$  and  $K$  are multi-allelic microsatellites when compared to the biallelic SNPs in the onset of association mapping (Zhu et al. 2008; Yang et al. 2011). Zhu et al. (2008) further argued that a good starting point for simple sequence repeat (SSR) marker number can be four times the chromosome number of the species.

Melon is an important desert fruit with tremendous diversity that is a product of consumer preferences from different countries, ecologies and cultures. Understanding footprints of divergence and genomic footprints of adaptation underlying the formation of various morphotypes is very important to the development of disease-resistant and high-quality melons. A basic understanding of population structure and linkage disequilibrium (LD) is limited and has lags behind that of other crops. Characterization of population structure and LD are paramount for association mapping of the QTL that underlie various complex traits (Yu and Buckler 2006). The distribution pattern of LD across the genome directly depends on evolutionary forces such as genetic drift, population structure, levels of inbreeding across the genome and the map regions contributing genetic differentiation among the subpopulations. Emergence and maintenance of LD is based on such evolutionary forces and pattern of selection (Ersoz et al. 2007; Xiao et al. 2012).

We used mapped single locus SSRs to resolve population structure in diverse melon accessions, as this research is the first that has adapted association

mapping in melons. As genomic technologies continue to evolve, high-density coverage of SNPs will be feasible in the near future. Currently genome-wide SNPs could be resolved only for a limited set of melon accessions. When compared to the other marker systems such as SNPs, SSRs are relatively new alleles and exhibit higher rates of mutation, increasing the opportunity for unique length variants to have arisen after domestication (Remington et al. 2001). Consequently, the SSR-derived datasets can resolve the most recent population structure when compared to SNPs (Flint-Garcia et al. 2005).

This current study aimed to resolve the genetic diversity and relatedness of eastern European melon germplasm with the melons of Asia and the western hemisphere using microsatellite markers that are mapped to various linkage groups. Our other objective was to compare LD among the three groups (Eastern Europe, Asia and Euro-North American) across the linkage groups and to perform association mapping for various fruit traits.

## Materials and methods

Thirty-eight accessions of melons belonging to a wide geographical region of Eastern Europe were included for the molecular diversity analysis along with 24 accessions of *cantalupensis*, three *inodorus*, and 22 Asian collections, *makuwa*, *dudaim* and *memordica* (Table 1). Eighty-seven accessions that were previously selfed for the three seasons were grown in three replications during three seasons (2005–2007) using a row-to-plant spacing of 140 × 70 cm. Twenty plants per accession were grown per replication. Data were collected pertaining to fruit weight (kg), fruit length (cm), fruit diameter (cm), fruit shape (the ratio of fruit length and diameter), soluble solids concentration (measured as % Brix with a hand-held refractometer manufactured by Atago Co. Ltd.), flesh thickness (cm) and rind pressure in kg/mm<sup>2</sup> (measured using a FT 011 penetrometer).

### Marker resources

The 268 single-locus SSRs used in the study are from various linkage groups of a published consensus map (Diaz et al. 2011). SSRs that had several nonspecific bands and SSRs with multiple loci were carefully

**Table 1** List of accessions used in the current study

No.	Accession	Country	Type
1	Gorkovskaia310	Russia	<i>adana</i>
2	Kubanka93	Russia	<i>adana</i>
3	Lipneva	Ukraine	<i>adana</i>
4	Titovka-Original	Ukraine	<i>adana</i>
5	Pepsha	Russia	<i>adana</i>
6	Titovka 1R_DASU	Ukraine	<i>adana</i>
7	Samarskaia	Ukraine	<i>adana</i>
8	Titovka zap	Ukraine	<i>adana</i>
9	Titovka s/e	Ukraine	<i>adana</i>
10	Ingulka	Ukraine	<i>adana</i>
11	Titovka1R	Ukraine	<i>adana</i>
12	Gruntovaia gribovskaia	Russia	<i>adana</i>
13	Ananas	Ukraine	<i>adana</i>
14	Selena	Ukraine	<i>adana</i>
15	Zlata	Ukraine	<i>adana</i>
16	Lada	Ukraine	<i>adana</i>
17	Tavrichanka	Ukraine	<i>adana</i>
18	Kolhoznitza	Russia	<i>adana</i>
19	G14	Ukraine	<i>adana</i>
20	Dachnitza	Ukraine	<i>adana</i>
21	Dneprianka163	Ukraine	<i>adana</i>
22	ZhZL	Ukraine	<i>adana</i>
23	Bronzovka	Russia	<i>adana</i>
24	Kzht	Ukraine	<i>adana</i>
25	Desertnaia5	Russia	<i>adana</i>
26	KRL	Ukraine	<i>adana</i>
27	N38	Russia	<i>adana</i>
28	Ineia	Ukraine	<i>adana</i>
29	Serpianka	Ukraine	<i>adana</i>
30	Beregina	Ukraine	<i>adana</i>
31	Promitey	Ukraine	<i>adana</i>
32	Diana	Ukraine	<i>adana</i>
33	Musa	Ukraine	<i>adana</i>
34	Zolotistaia	Russia	<i>adana</i>
35	L20/1	Ukraine	<i>adana</i>
36	L22/1	Ukraine	<i>adana</i>
37	Rannia133	Russia	<i>adana</i>
38	Krinichanka	Ukraine	<i>adana</i>
39	Amarillo Oro	Spain	<i>inodorus</i>
40	Honey Dew Green Flesh	USA	<i>inodorus</i>
41	Schoon's hardshell	USA	<i>cantalupensis</i>
42	Planter,s jumbo	USA	<i>cantalupensis</i>
43	Minnesota midget	USA	<i>cantalupensis</i>
44	Iroquois	USA	<i>cantalupensis</i>

**Table 1** continued

No.	Accession	Country	Type
45	Banana	USA	<i>cantalupensis</i>
46	Small Persian	USA	<i>cantalupensis</i>
47	Top mark	USA	<i>cantalupensis</i>
48	Hales Best Jumbo	USA	<i>cantalupensis</i>
49	Eden Gem	USA	<i>cantalupensis</i>
50	Ananas Improved	USA	<i>cantalupensis</i>
51	Edisto	USA	<i>cantalupensis</i>
52	Rocky Ford Green Flesh	USA	<i>cantalupensis</i>
53	Honey Rock	USA	<i>cantalupensis</i>
54	Queen Anne's Pocket	USA	<i>dudaim</i>
55	Noir des Carmes	France	<i>cantalupensis</i>
56	Sierra Gold	USA	<i>cantalupensis</i>
57	Jenny Lind	USA	<i>cantalupensis</i>
58	Yellow Canary	Spain	<i>inodorus</i>
59	Emerald Gem	USA	<i>cantalupensis</i>
60	Kansas	USA	<i>cantalupensis</i>
61	Amish	USA	<i>cantalupensis</i>
62	Tip Top	USA	<i>cantalupensis</i>
63	Edisto 47	USA	<i>cantalupensis</i>
64	Plum Granny	USA	<i>dudaim</i>
65	Delicious 51	USA	<i>cantalupensis</i>
66	Old Original Israel	Israel	<i>cantalupensis</i>
67	Charentais	France	<i>cantalupensis</i>
68	K-5886	China	<i>makuwa</i>
69	K-5889	China	<i>makuwa</i>
70	K-5582	China	<i>makuwa</i>
71	K-1088	NA	<i>makuwa</i>
72	Diabo	Vietnam	<i>makuwa</i>
73	K-5578	China	<i>makuwa</i>
74	K-2886	China	<i>makuwa</i>
75	K-2668	India	<i>momordica</i>
76	K-1086	India	<i>makuwa</i>
77	Raketa	Far East Russia	<i>makuwa</i>
78	Kynpou	Japan	<i>makuwa</i>
79	K-2805	India	<i>momordica</i>
80	K-6913	China	<i>makuwa</i>
81	K-5551	China	<i>makuwa</i>
82	K-4177	India	<i>makuwa</i>
83	K-5573	China	<i>makuwa</i>
84	K-5544	China	<i>makuwa</i>
85	K-5543	China	<i>makuwa</i>
86	K-5006	China	<i>makuwa</i>
87	K-5360	China	<i>makuwa</i>

eliminated from the study. Thirty-two of the primer combinations were from the linkage group (LG) 1 that spanned a length of 99 cM, along with 11 from LG2 of length 94 cM, 19 from LG3 of length 95 cM, 40 from LG4 of length 119 cM, 14 from LG5 of length 110 cM, 27 from LG6 of length 98 cM, 24 from LG7 of length 99 cM, 28 from LG8 of length 123 cM, 11 from LG9 of length 84 cM, 16 from LG10 of length 73 cM, 20 from LG11 of length 80 cM and 26 from LG12 of length 76 cM.

#### DNA isolation and PCR conditions

The genomic DNA isolation was carried out using the procedure of Nimmakayala et al. (2009). The PCR reaction consisted of 200 ng of genomic DNA, 0.20  $\mu$ M of mixed forward and reverse primers, 1 $\times$  Buffer (10 mM Tris–HCl pH 8.2, 50 mM KCl, Triton 0.1 %, BSA 1 mg/ml), 1.5 mM MgCl<sub>2</sub>, 0.2 mM dNTPs and 1 U *Taq* polymerase in 10  $\mu$ L reaction volumes. Amplification was performed in a GeneAmp PCR 9700 System thermal cycler (Applied Biosystems Inc.) programmed to 94 °C for 2 min followed by 35 cycles of 94 °C for 30 s, 50–65 °C for 30 s, 72 °C for 1 min, and a final extension step at 72 °C for 10 min. Amplified products were separated on 3.5 % SFR-grade agarose gels. In scoring, stutters were avoided and discernible bands were scored as alleles. Allele sizes were estimated for the survey panel based on comparison with a 50-bp molecular weight ladder that was loaded twice on each SFR-grade agarose gel.

#### Data analysis

##### *Molecular genetic diversity, neutrality and gene flow*

The genetic variance was partitioned between and among the melon groups using the analysis of molecular variance (AMOVA) in the program Arlequin 2.0 (Schneider et al. 2000). Molecular genetic diversity was estimated using Nei's (1973) genetic diversity and heterozygosity ( $h$ ).  $F_{IS}$  and  $F_{ST}$  were estimated based on Wright's  $F$  statistics (Weir and Cockerham 1984) using the program PopGene version 1.31 (Yeh et al. 1999). For each locus, polymorphism information content (PIC) was calculated using the Excel Microsatellite Toolkit (Park 2001). Analysis of gene flow ( $N_m$ ) based on the private allele method (Slatkin 1985) was estimated using the program

Genepop version 4.1 (Rousset 2008). The Ewens–Watterson test (Manly 1985) uses the significantly different observed and expected Hardy–Weinberg homozygosities assuming that various loci are at mutation–drift equilibrium. Fluctuation in the distribution of observed  $F$  when compared to the mean is suggestive of balancing selection (if above mean) or selective sweep (if below mean) and even distribution if the populations are under equilibrium. The Ewens–Watterson neutrality test (Ewens 1972; Watterson 1978) was performed using Manly’s algorithm (1985) implemented in the software PopGene version 1.31 (Yeh et al. 1999) to investigate neutrality across the linkage groups. This is to test whether the observed homozygosity, calculated as the sum of squared allele frequency, is significantly higher or lower than the expected homozygosity based on simulation under neutrality expectations. This approach could suggest whether selection is in operation on a particular genomic region across the linkage groups (Ejmond et al. 2010; Xiao et al. 2012).

#### *Population structure analysis and validation*

Structure version 2.2 (Pritchard et al. 2000) which calculates posterior probability of the data for a given  $K$ ,  $\Pr(X|K)$  was used to cluster individuals into  $K$  groups. The number of populations ( $K$ ) was determined following the admixture model with correlated alleles, with a  $K$  of 2–20. Five independent runs of 50,000 Markov chain Monte Carlo (MCMC) generations and 50,000 generations of burn-in were used for each value of  $K$ . The optimal  $K$  value was determined by the posterior probability [ $\ln P(D)$ ] and an ad hoc statistic  $\Delta K$  based on the rate of change in [ $\ln P(D)$ ] between successive  $K$  (Evanno et al. 2005). The number of  $K$ s in each dataset was evaluated using  $\Delta K$  values according to Evanno et al. (2005) using the software Structure Harvester.

#### *Linkage disequilibrium*

LD was estimated as the  $r^2$  between all the pairs of SSRs with 1,000 permutations using the package TASSEL version 2.2 (<http://www.maizegenetics.net>) (Bradbury et al. 2007). Rare alleles with allele frequency of 0.5 and less were removed from the dataset before analysis. LD was estimated for global, linked and unlinked markers. The 99th percentile of  $r^2$

distribution for unlinked markers was considered as the background level of LD, which determined whether LD is due to physical linkage (Mather et al. 2007). The decay of LD along with the map distance was estimated according to Mather et al. (2007). LD decay over genetic distance was investigated by plotting pair-wise  $r^2$  values against genetic distance (cM) between the markers. To visualize LD throughout the genome, heatmaps were produced based on the  $P$  values of pair-wise  $r^2$  estimates of all marker pairs. These heatmaps were used to identify LD blocks in various melon groups at specific map locations.

#### *Association mapping*

The marker set after removing minor allele frequencies was used to estimate a kinship ( $K$ ) matrix using the software TASSEL 2.1 that uses the proportion of alleles shared between each pair of accessions in the study. The  $Q$  matrix was adapted from the  $K$ -3 cluster result of the analysis obtained from Structure version 2.2. A mixed linear model (MLM) can significantly reduce the spurious marker–trait associations (Type I error showing false positives) resulting from population structure, as  $Q$  and  $K$  are used as covariants in the analysis. A false discovery rate (FDR) of 0.05 was used as a threshold for significant association using highly stringent Bonferroni correction (Sidak 1967) as well as moderate Benjamini and Hochberg correction (1995).

## **Results**

### Phenotypic data and correlations of fruit traits

Phenotypic data recorded on 87 accessions for three different seasons is presented in Supplementary Table 1. The highest heritability (broad sense) was noted for fruit shape (0.82) and fruit diameter (0.81) when compared to the other traits. The lowest heritability (0.56) was recorded for the trait fruit weight. Significant positive correlation was noted between fruit weight and flesh thickness (0.79), fruit length (0.75) and fruit diameter (0.87). Flesh thickness was also noted to be in positive association with fruit diameter (0.82) and fruit length (0.66). Fruit shape and fruit length were significantly associated with a correlation coefficient of 0.66. Soluble solids content

and rind pressure were not correlated with any of the other traits in the study (Supplementary Table 2).

#### Allele frequency, gene flow and molecular genetic diversity among the melon collections

Analysis of molecular variance of the three groups of eastern European (EE or *adana*), CI (*cantalupensis* and *inodorus*) and Asian (*makuwa*, *dudaim* and *memordica*) accessions indicated highly significant differences ( $P \leq 0.0001$ ) across (17.52 % of variance) and within (68.08 % of variance) groups. Allele numbers amplified ranged from 2 to 10. Nei's expected heterozygosities are better indicators of divergence and are presented in Supplementary Fig. 1. PIC (polymorphic information content) values were in the range of 0.7–0.88 for 49 loci, 179 loci had PIC values in the range of 0.4–0.69 and the rest of them were below 0.4 (Supplementary Fig. 2). The distributions of  $F_{ST}$ , which is population genetic differentiation, and  $F_{IS}$ , an indicator of inbreeding depression or fixation index, are presented across the entire linkage map in Fig. 1. Twenty-four loci had  $F_{ST}$  in the range of 0.3–0.64, indicating that these markers contributed the majority of the divergence among the three groups, 106 loci had  $F_{ST}$  in the range from 0.1 to

0.29 and the rest of them were below 0.1.  $F_{IS}$  was above 0.9 for 128 loci, indicating that these loci are fixed among the three groups (Fig. 1). Genetic divergence (Nei 1973) analysis indicated that EE and CI diverged by 20 %, EE and Asian 15 % and CI and Asian 23 %. The neighbor-joining (NJ) tree based on Nei's genetic diversities resolved three robust clusters with some exceptions, of which *adana* is notable in the middle position in the tree and further split into two subclusters, and on the top and bottom of the tree were clusters of Asian and CI groups, respectively (Fig. 2). The CI cluster had two subclusters of which one is purely *cantalupensis* and the other is a mixed group containing accessions from *cantalupensis*, both the *inodorus* that are in the study, Pepsha of *adana* and K-5886 of *makuwa*. The middle *adana* group had the first subcluster, which is predominantly *adana* type containing cultivars that are early (known as *europaeus*) and mid-maturity (*aestivalis*) types. The second subcluster of *adana* group was with rest of the *aestivalis* and winter accessions (late maturity and known as *haemalis*) along with a mixture of various other morphotypes, viz. Rocky Ford Green flesh (USA), Charentais (France) and Old original Israel (Israel) of *cantalupensis*, both the *dudaim* types in the study (Plum Granny and Queen Anne's Pocket of

**Fig. 1** Distribution pattern of  $F_{ST}$  and  $F_{IS}$  across the length of the melon genetic map

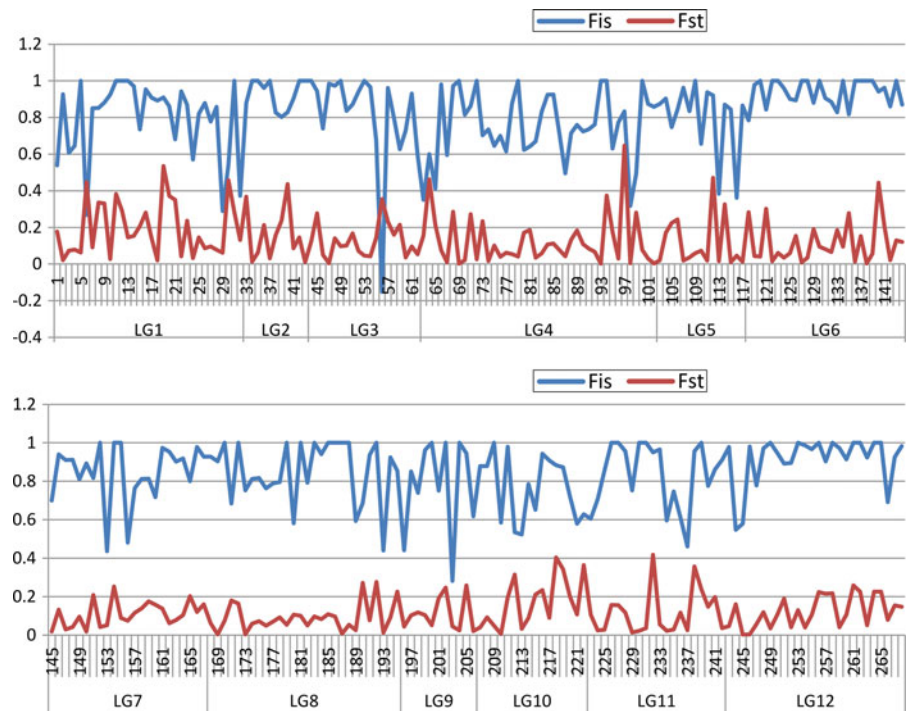


**Fig. 2** Molecular genetic relationships as depicted on neighbor-joining tree and population structure among melon accessions (numbers on top of tree clusters are bootstrap values)

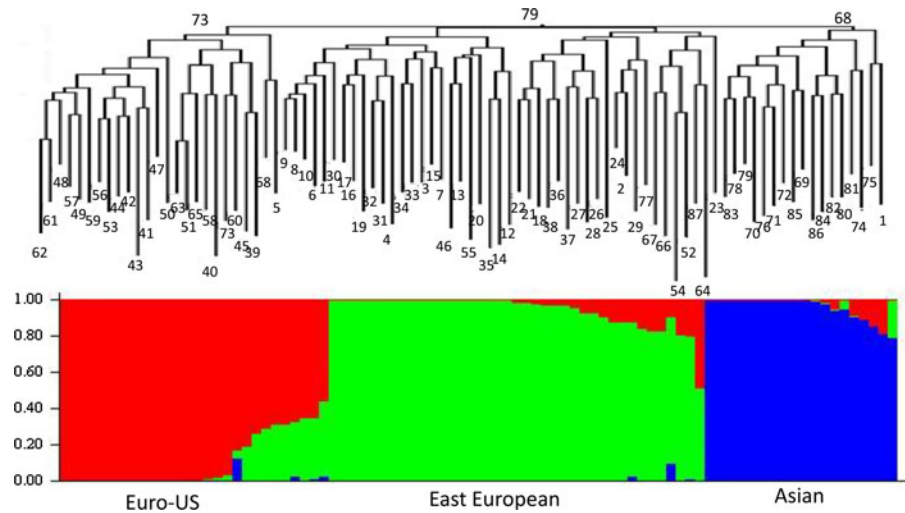
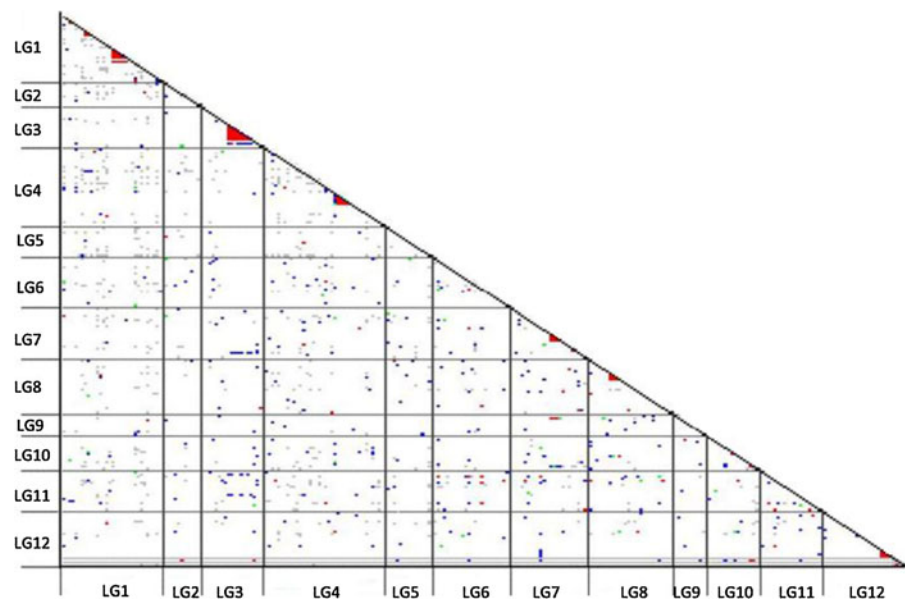


**Fig. 3** LD pattern in *adana* group of melons



USA) and K-5360 (China) and Raketa (a collection from far east Russia) of *makuwa*, clustered at the bottom of second subcluster of *adana*. The NJ tree had a third cluster predominantly with *makuwa* and *momordica* from China and India with the sole exception of Gorkovskaia310 of *adana* group. The population structure analysis revealed that *K-3* is the most appropriate grouping that can be assumed as it had the highest  $\Delta K$  (Supplementary Fig. 3). The  $N_m$  estimates (private allele method) is to identify private alleles and number of migrant alleles per population (Barton and Slatkin 1986). This test revealed that the mean frequency of private alleles  $p(1) = 0.107956$

per group and number of migrant alleles ( $N_m$  indices) ranged from 0.13 to 19.1 with an average of 7.72 per locus. An overall Ewens–Watterson test for neutrality was carried out for all the linkage groups to understand the genomic regions which are under selection sweep (Supplementary Fig. 4). A comprehensive view of melon genetic diversity and its footprints can be appreciated after taking into consideration the collective distribution of  $F_{ST}$ ,  $F_{IS}$  and selection sweep across various linkage groups. For example, linkage group 12 has undergone remarkable selection sweep (the curve of the observed mean is significantly below the curve of the mean in Supplementary Fig. 4) when compared

to the other linkage groups, where observed  $F$  is often fluctuating above the mean. Intriguingly,  $F_{ST}$  distribution for LG12 is the lowest of all linkage groups and was in the range of 0–0.2 throughout, which indicates that the markers on this LG contributed less to population genetic differentiation because of selection sweep. In contrary,  $F_{IS}$  distribution across LG12 was the highest, implying fixation of alleles and inbreeding (Fig. 1).

#### Distribution of linkage disequilibrium across various groups

The total of significant LDs was 3,405 (based on  $r^2$ ,  $P < 0.05$ ) out of 35,778 pairs, which includes both inter- and intrachromosomal combinations. The extent of LD was significant among 425 marker pairs (based on  $r^2$ ,  $P < 0.05$ ) out of 1,342 intrachromosomal pairs of SSR loci, which is 31.7 %. LD decay in melon varies across the linkage groups when diverse melons of all the three groups are included. However, a general trend can be drawn using the LOESS line, which indicated a sharp fall of LD at 5 cM. To start with we defined a base line at which the significant LD values intercept the LOESS curve and defined the mapping distance at which LD decays in melon. LD decay for the entire collection is at 5 cM (Supplementary Fig. 5) and for individual groups 5, 5 and 4 cM for EE, CI and Asian, respectively. LD distribution patterns across various linkage groups as represented by  $P$  values of marker associations of *adana* group is presented as a heatmap (Fig. 3) and similar heatmaps for the CI and Asian groups are in Supplementary Figs. 7 and 8. Position and length of significant LD blocks present across the melon LGs among various groups are presented in Supplementary Table 3.

The third block of LG1 was at 55 cM and spread across 3 cM between the markers TJ26 and ECM58. Linkage group 1 was noted to have three major LD blocks, of which the first block in Eastern European and Asian groups spans 1 cM and is between the markers CMAAGN207 and CMAAGN221 located at the 8 cM position of LG1. This corresponding block in the CI group is larger than the other groups spanning between 7 and 9 cM positions of LG1 for 2 cM and is located between the markers ESM163 and CMAAGN221. A second block of the EE group was detected at 36 cM of LG1 and further spread across 4 cM and located between the markers CMN53\_36

and CMCTN86 and was larger than the corresponding block of the CI group. This block in CI was detected at 36 cM of LG1 spread across 2 cM between the markers CMN53\_36 and CMN23\_44. Intriguingly, this block is absent in the Asian group. A third block of LG1 in the EE group was at 55 cM and spread across 3 cM between the markers TJ26 and ECM58. In contrast, this block in the CI group was at 56 cM and spread across 1 cM between the markers TJ26 and CMMS4\_3. The corresponding block in the Asian group is located around 57 cM and between CMMS4 and CMN22\_22, which is clearly a weaker and smaller block with reduced significance of  $P < 0.01$ .

In the current study, no LD block was detected on LG2. The block on LG3 in the EE group was located at the 41 cM position between CMBR083 and CMBR056 spanning up to the 45 cM position, which is slightly smaller than the block of CI and Asian. Corresponding blocks in CI and Asian were located at the 41 cM position between CMBR083 and CMBR018 spanning up to the 46 cM position. Locus CMBR100 decayed at the middle LD block in the Asian group. LG4 has one major block at the 71 cM position with the size of 1 cM in EE and CI groups, located between CMBR094 and CMBR104. Its corresponding block in the Asian group is exactly the same size but decayed in the middle at CMBR072. LG5 has a block at 26 cM of LG5 spanning 3 cM distance and located between CMAGN61 and CMAGN52 in CI only. A block at 77 cM of LG6 with flanking markers CMBR143 and CMBR108 was located in CI and Asian groups, which is completely absent in the Eastern European accessions.

Current study detected two discernible blocks on LG7, of which one is located at 56 cM and spread up to 58 cM between CMATCN184 and CMAGN141. The second block of LG7 was located between the 65 and 66 cM positions with flanking markers CMBR021 and CMGAN21. The current study detected two blocks on LG7, of which one is located at 57 and 58 cM between CMBR053 and CMBR027 in the EE group. The corresponding blocks in CI and Asian were located between 56 and 57 cM between CMBR012 and CMBR027. The second block of LG7 in all the three groups was located at the 65 cM position with flanking markers CMBR021 and CMBR084. The LD block on LG8 is located at the 16 cM position between CMBR109 and CMBR098, which is same in all the three groups that were studied in the current research. LG9 had one block in the Asian group at 38 cM, which



was spread up to 42 cM with flanking markers CMN04\_19 and DM0030 at either side. This block was completely absent in the EE and CI groups. Two blocks were detected on LG10. The first block of EE and CI is of 1 cM size and located at the 27 cM position and found between CMBR055 and MU6549. The longest second block of LG10 was at 52 and 56 cM with flanking markers CMCT134B and CMTC134 and was present in all the three groups. Out of two blocks of LG12, one was at 38 cM between CMN62\_03 and CMN09\_76 and present only in the Asian group. The other block on LG12 was seen at 61 cM between the markers CMCTTN259 and CMBR051, in exactly similar orientation among all the three groups of melons.

### Diversity of phenotypic traits

#### *Association mapping to locate QTL for various fruit traits*

A MLM was used in the current study to locate QTL for three consecutive years. Marker significance was adjusted using Bonferroni's correction. For 268 tests at an alpha of 0.05, the adjusted  $P = 0.0002206$ , and for alpha of 0.01 the adjusted  $P = 4.41E-5$ . Lists of markers that are linked to various traits are given along with their corresponding  $R^2$  and  $P$  values across all the years in Table 2. A majority of the QTL detected are repeated across years, indicating the robustness of the identified QTL. Among the major QTL, for the trait fruit shape, which is estimated as a ratio of fruit length and width, CMN-21\_82 and CMBR061 of LG4 located at 42 and 47 cM, respectively, could explain around 50 % of the variation in two consecutive years and CMBR27 of LG7 explained 14 % in one year. MU3594 of LG8 was linked with a  $R^2$  value of 0.7441–0.893 in all 3 years. This marker is highly significant and could withstand Bonferroni cut-off. The same marker revealed highly significant association with fruit length (with  $R^2$  values of 0.257, 0.3546 and 0.3856) for all three years. As the fruit length is one of the contributing traits to estimating fruit shape, the common association of MU3594 with both the traits reveals the cogency of the current research. Five QTL were detected for fruit diameter on chromosomes 1, 6, 7, and 11 with a cumulative contribution that amounts to 41 % of the total variation. Soluble solids is another important trait which was studied all the

three years and in the current study; seven different markers cumulatively explained about 25 % of the variation. Two strong QTL were detected for rind pressure.

### Discussion

Our study provides useful information pertaining to morphological and molecular characterizations of melons specific to *adana* collections in relation to the other world collections. The eastern European melon group, which is an *adana* morphotype known for its sweetness and high flavor, contains diverse accessions and consists of the subgroups *aestivalis*, *europaeus* and *hiemalis* which are heterogenous but can be distinguished. Desetnaia 5, Dachnitsa, Lipneva, Pepsha and Samarskaia are predominantly *aestivalis* group and have furrowed fruits. The fruit color of *aestivalis* varies from green to dark green in color while immature, changing to a yellowish brown at maturity. The *europaeus* group had accessions with netted fruit surfaces with white colored flesh and is predominantly early-type (Nimmakayala et al. 2009). The subgroup *hiemalis* is a non-climacteric fruit and hence possesses long shelf life. Another distinguishing feature is the diversity in sex expression within the *adana* morphotype. The sex expression in *europaeus* and *hiemalis* groups is andromonecious or mononecious, whereas in *aestivalis*, the majority of collections are andromonecious (Tomason 2002). Melon groups *cantalupensis* and *inodorous* have sweet flesh and are cultivated in Europe and the USA. Groups *momordica*, *dudaim* and *conomon* have low-sugar flesh with smooth skin, small seed type and are cultivated in South and East Asia (Akashi et al. 2002; Tanaka et al. 2007). Similar to the results of the current study, melon accessions were classified by several researchers using molecular markers into Euro-American melons (*cantalupensis* and *inodorous*) and Asian melons (Silberstein et al. 1999; Stepansky et al. 1999; Staub et al. 2000; Tanaka et al. 2007) with the comparable genetic divergence. The current study revealed that the eastern European types are genetically close to Asian types and the Asian and EE types are more diverse than the CI group. Sebastian et al. (2010), after studying various African and Asian species, concluded that Asia is the center of origin for melon and as such it contains enormous genetic

**Table 2** List of markers linked to various traits and their  $R^2$  and associated  $P$  value

Marker	LG	2005		2006		2007	
		$R^2$	$P$ value	$R^2$	$P$ value	$R^2$	$P$ value
<i>Fruit weight</i>							
TJ29	12	0.01	3.26E–05**	–	–	–	–
CMN01_15	2	–	–	0.0718	9.80E–04*	–	–
CMBR105	3	0.02	4.1E–04*	0.03	2.06E–05**	0.03	1.34E–05**
<i>Fruit shape</i>							
CMCTN4	1	–	–	0.095	7.91E–09**	–	–
CMBR105	3	0.01	2.08E–08*	0.0174	1.21E–07**	0.0119	2.1E–04*
TJ30	3	–	–	0.1083	9.60E–05*	–	–
CMN21_82	4	–	–	0.5005	8.82E–04*	0.4963	6.04E–05*
CMBR027	7	0.148	1.68E–07*	0.0134	4.06E–04*	–	–
CMTCN30	7	–	–	–	–	0.598	7.29E–06**
MU3594	8	0.893	1.62E–18**	0.7441	3.48E–05**	0.7477	0.0078
DM0431	9	0.034	1.50E–04*	0.0374	1.91E–05**	0.0372	8.59E–05**
CMATN121	11	–	–	–	–	0.0382	1.54E–06**
<i>Fruit length</i>							
CMAAGN221	1	–	–	–	–	0.0674	3.13E–04*
GCM168	1	–	–	–	–	0.3222	1.87E–05**
CMGT108	2	0.044	2.28E–04*	–	–	0.018	0.0021
CMBR105	3	0.021	2.91E–06**	–	–	0.0118	2.22E–06**
CMBR056	3	–	–	0.0825	0.81E–04*	–	–
CMN06_19	4	–	–	0.0425	8.67E–05*	0.0634	5.17E–04*
CMBR061	4	–	–	–	–	0.3031	3.71E–05**
CMBR027	7	0.046	2.59E–04*	–	–	–	–
CMTCN30	7	–	–	–	–	0.3768	1.05E–04*
CMN_C05	8	0.042	9.58E–05*	–	–	–	–
MU3594-3	8	0.257	9.77E–05*	0.3546	1.30E–04*	0.3856	8.22E–07**
CMN61_44	12	–	–	–	–	0.1712	8.37E–04*
<i>Fruit diameter</i>							
CMMS27	1	0.099	4.73E–07**	–	–	0.0811	3.5E–04*
TJ3	1	0.107	9.81E–05*	–	–	–	–
CMBR139	6	0.062	5.76E–04*	–	–	–	–
CMMS30_3	7	–	–	0.0452	3.04E–04*	0.0303	1.61E–04*
<i>Soluble solids</i>							
CMBR105	3	0.053	7.6E–04*	0.1	2.94E–07**	–	–
CMBR001	3	–	–	–	–	0.0554	7.79E–06**
TJ30	3	0.01	2.05E–05*	–	–	–	–
CMN06_19	4	0.123	5.31E–05*	0.2756	1.72E–04*	–	–
CMBR104	4	–	–	–	–	0.1548	5.46E–04*
MU7161	6	0.077	6.28E–04*	–	–	–	–
CMBR024	8	–	–	0.074	3.73E–04*	0.068	3.44E–04*
ECM56	9	–	–	–	–	0.0102	2.67E–06**
<i>Rind pressure</i>							
CMGT108	2	–	–	–	–	0.1727	1.93E–04*

**Table 2** continued

Marker	LG	2005		2006		2007	
		$R^2$	$P$ value	$R^2$	$P$ value	$R^2$	$P$ value
CMBR105	3	0.12	1.59E–04*	0.0905	8.27E–05*	0.0514	6.41E–07**
CMN06_19	4	0.031	8.38E–06**	–	–	0.0948	1.80E–04*
CMN04_01	7	0.214	1.7E–04*	–	–	0.1727	2.80E–04*
<i>Thickness</i>							
MU3752	1	0.013	0.87E–04*	0.0228	1.82E–05**	0.0145	4.4E–04*
CMBR105	3	0.044	3.9E–04*	0.0553	8.13E–06**	0.0451	1.33E–05**

Significant \*\* Bonferroni correction, \* Benjamini correction

diversity. Blanca et al. (2012) and Nimmakayala et al. (2009) considered *adana* type to be ancestral to *cantalupensis* group. The variability found in this group can be effectively used for introgression into the CI group as this is a relatively underexploited reservoir of genetic variability for improving disease resistance, yield and fruit quality.

This study is the first attempt at detecting LD in the melon genome. The common occurrence of several LD blocks across the three melon groups suggests that LD mapping is feasible for locating genes underlying complex traits in the diverse melon germplasm. Polymorphic SSRs used in the current study were found to be very valuable for evaluating population structure among the three groups of melons used in the current study. Similar to our study, SSRs proved to be very useful for accurately resolving population structure in many other crops (Maccaferri et al. 2010; Huang et al. 2002; Matsuoka et al. 2002; Garris et al. 2005; Liu et al. 2012; D'hoop et al. 2010; Jin et al. 2010; Malysheva-Otto et al. 2006; Zhang et al. 2011). Microsatellite markers generally have higher power than SNPs even if large numbers of SNPs are used (Ohashi and Tokunaga 2003) for initial genome-wide screening, and SNPs should be used for fine-scale mapping after the screen.

A MLM was used in the current study for three consecutive years to locate QTL with the subsequent correction using Bonferroni's method. The most intriguing part of the current study is that many of the QTL previously published using the recombinant mapping approach could be validated. Validation of the QTL identified by the other researchers makes the current study robust and very reliable. We summarized all the QTL identified in the current study and

validated them by comparing previous studies using the recombinant mapping approach in Supplementary Table 4. For example, Eduardo et al. (2007) characterized a near-isogenic line population developed from the cross Piel de Sapo × PI161375 to locate QTL for fruit shape on linkage groups 1 (CMCCA145 at 52 cM and CMCTN4 at 99 cM), LG3 (CSWCT10 at 29 cM and TJ10 at 84 cM), LG7 (CMAGN75 at 38 cM and CMGA15 at 96 cM), LG9 (CMCT47 at 14 cM and CMCTN7 at 62 cM) and LG11 (CMCT160a at 10 cM and CMGA104 at 61 cM) positions. In the current study, the fruit shape QTL identified linked to CMCTN4 at 99 cM of LG1, CMBR105 at 42 cM of LG3, between CMBR27 at 57 cM of LG7, DMO431 at 44 cM of LG9, CMATN121 at 53 cM of LG11 are the same markers or the markers that are located near the markers identified by Eduardo et al. (2007). For fruit diameter, QTL identified by Zalapa et al. (2007), Paris et al. (2008), Harel-Beja et al. (2010) and Xu (unpublished) are the same markers identified in the current study. For fruit length, the QTL positions identified by Eduardo et al. (2007) and Harel-Beja et al. (2010) are the same as in the current study. QTL positions for fruit weight identified by Eduardo et al. (2007) and Harel-Beja et al. (2010) are again comparable to positions identified in the current study. Four QTL linked to soluble solids content were in the same position identified by Eduardo et al. (2007) and one QTL that was previously located by Monforte et al. (2004) could be revalidated in the current study. Minor discrepancies in the position, strength and the variation explained by the QTL can be bridged if more melon groups and accessions are involved in future studies combined with high-throughput marker panels. Results pertaining to selection sweep and further

resolution of LD can be more accurately predicted when high-throughput marker panels such as SNPs are used on a larger set of diverse melon accessions.

**Acknowledgments** The authors are grateful to Drs. Hankins, Malkaram and Barry for critical review of the manuscript. Funding support is provided by Gus R. Douglass Institute (Evans Allen Project to Nimmakayala) and USDA-NIFA Research (2007-03466, 2010-02247 and 2012-02511).

## References

- Akashi Y, Fukuda N, Wako T, Masuda M, Kato K (2002) Genetic variation and phylogenetic relationships in East and South Asian melons, *Cucumis melo* L., based on the analysis of five isozymes. *Euphytica* 125:385–396
- Arumuganathan K, Earle ED (1991) Estimation of nuclear DNA amounts of plants by flow cytometry. *Plant Mol Biol Rep* 9(3):229–241
- Barton NH, Slatkin M (1986) A quasi-equilibrium theory of the distribution of rare alleles in a subdivided population. *Heredity* 56:409–415
- Benjamini Y, Hochberg Y (1995) Controlling the false discovery rate: a practical and powerful approach to multiple testing. *J R Stat Soc* 57:289–300
- Blanca J, Esteras C, Ziarsolo P, Perez D, Fernandez V, Collado C, Rodriguez R, Ballester A, Roig C, Canizares J, Pico B (2012) Transcriptome sequencing for SNP discovery across *Cucumis melo* L. *BMC Genomics* 13(1):280
- Bradbury PJ, Zhang Z, Kroon DE, Casstevens TM, Ramdoss Y, Buckler ES (2007) Tassel: software for association mapping of complex traits in diverse samples. *Bioinformatics* 23:2633–2635
- Decker-Walters DS, Chung SM, Staub JE, Quemada HD, López-Sesé AI (2002) The origin and genetic affinities of wild populations of melon (*Cucumis melo*, Cucurbitaceae) in North America. *Plant Syst Evol* 233(3):183–197. doi: [10.1007/s00606-002-0191-3](https://doi.org/10.1007/s00606-002-0191-3)
- Deleu W, Esteras C, Roig C, Gonzalez-To M, Fernandez-Silva I, Gonzalez-Ibeas D, Blanca J, Aranda M, Arus P, Nuez F, Monforte A, Pico M, Garcia-Mas J (2009) A set of EST-SNPs for map saturation and cultivar identification in melon. *BMC Plant Biol* 9(1):90
- Diaz A, Fergany M, Formisano G, Ziarsolo P, Blanca J, Fei Z, Staub JE, Zalapa JE, Cuevas HE, Dace G, Oliver M, Boissot N, Dogimont C, Pitrat M, Hofstede R, Koert P, Harel-Beja R, Tzuri G, Portnoy V, Cohen S, Schaffer A, Katzir N, Xu Y, Zhang H, Fukino N, Matsumoto S, Garcia-Mas J, Monforte AJ (2011) A consensus linkage map for molecular markers and Quantitative Trait Loci associated with economically important traits in melon (*Cucumis melo* L.). *BMC Plant Biol* 11:111. doi: [10.1186/1471-2229-11-111](https://doi.org/10.1186/1471-2229-11-111)
- D'hoop B, Paulo M, Kowitwanich K, Sengers M, Visser R, Eck H, Eeuwijk F (2010) Population structure and linkage disequilibrium unraveled in tetraploid potato. *Theor Appl Genet* 121:1151–1170
- Eduardo I, Arús P, Monforte AJ, Fernández-Trujillo JP, Obando J, Martínez JA, Alarcón A, Álvarez JM, Van Der Knaap E (2007) Estimating the genetic architecture of fruit quality traits in melon (*Cucumis melo* L.) using a genomic library of near-isogenic lines. *J Am Soc Hortic Sci* 132:80–89
- Ejmsmond MJ, Babik W, Radwan J (2010) MHC allele frequency distributions under parasite-driven selection: a simulation model. *BMC Evol Biol* 10:332. doi: [10.1186/1471-2148-10-332](https://doi.org/10.1186/1471-2148-10-332)
- Ersoz ES, Yu J, Buckler ES (2007) Applications of linkage disequilibrium and association mapping in crop plants. In: Varshney RK, Tuberosa R (eds) *Genomics-assisted crop improvement*. Springer, Berlin, pp 97–119. doi: [10.1007/978-1-4020-6295-7\\_5](https://doi.org/10.1007/978-1-4020-6295-7_5)
- Evanno G, Regnaut S, Goudet J (2005) Detecting the number of clusters of individuals using the software structure: a simulation study. *Mol Ecol* 14:2611–2620
- Ewens WJ (1972) Sampling theory of selectively neutral alleles. *Theor Popul Biol* 3(1):87–112
- Flint Garcia SA, Thuillet A, Yu J, Pressoir G, Romero SM, Mitchell SE, Doebley J, Kresovich S, Goodman MM, Buckler ES (2005) Maize association population: a high resolution platform for quantitative trait locus dissection. *Plant J* 44:1054–1064
- Garris AJ, Tai TH, Coburn J, Kresovich S, McCouch S (2005) Genetic structure and diversity in *Oryza sativa* L. *Genetics* 169:1631–1638. doi: [10.1534/genetics.104.035642](https://doi.org/10.1534/genetics.104.035642)
- Harel-Beja R, Tzuri G, Portnoy V, Lotan-Pompan M, Lev S, Cohen S, Dai N, Yeselson L, Meir A, Libhaber S, Avisar E, Melame T, Van Koert P, Verbakel H, Hofstede R, Volpin H, Oliver M, Fougere A, Stalh C, Fauve J, Copes B, Fei Z, Giovannoni J, Ori N, Lewinsohn E, Sherman A, Burger J, Tadmor Y, Schaffer A, Katzir N (2010) A genetic map of melon highly enriched with fruit quality QTLs and EST markers, including sugar and carotenoid metabolism genes. *Theor Appl Genet* 121:511–533
- Huang Q, Beharav A, Li Y, Kirzhner V, Nevo E (2002) Mosaic microecological differential stress causes adaptive microsatellite divergence in wild barley, *Hordeum spontaneum*. *Genome Biol* 45:1216–1229
- Jeffrey C (1980) A review of the Cucurbitaceae. *Bot J Linn Soc* 81:233–247
- Jin L, Lu Y, Xiao P, Sun M, Corke H, Bao J (2010) Genetic diversity and population structure of a diverse set of rice germplasm for association mapping. *Theor Appl Genet* 121(3):475–487. doi: [10.1007/s00122-010-1324-7](https://doi.org/10.1007/s00122-010-1324-7)
- Liu W, Reif J, Ranc N, Porta G, Würschum T (2012) Comparison of biometrical approaches for QTL detection in multiple segregating families. *Theor Appl Genet* 125:987–998. doi: [10.1007/s00122-012-1889-4](https://doi.org/10.1007/s00122-012-1889-4)
- Maccaferri M, Sanguineti MC, Mantovani P, Demontis A, Massi A, Ammar K, Kolmer JA, Czembor JH, Ezrati S, Tuberosa R (2010) Association mapping of leaf rust response in durum wheat. *Mol Breeding* 26:189–228. doi: [10.1007/s11032-009-9353-0](https://doi.org/10.1007/s11032-009-9353-0)
- Manly BFJ (1985) The statistics of natural selection. *Spurious Test Results Due to Isolation By Distance*. Chapman & Hall, London, pp 186–195
- Malyshva-Otto L, Ganai M, Roder M (2006) Analysis of molecular diversity, population structure and linkage disequilibrium in a worldwide survey of cultivated barley germplasm (*Hordeum vulgare* L.). *BMC Genet* 7(1):6

- Mather K, Caicedo A, Polato N, Olsen K, McCouch S, Purugganan M (2007) The extent of linkage disequilibrium in rice (*Oryza sativa* L.). *Genetics* 177:2223–2232
- Matsuoka Y, Vigouroux Y, Goodman M, Sanchez GJ, Buckler E, Doebley J (2002) A single domestication for maize shown by multilocus microsatellite genotyping. *Proc Natl Acad Sci USA* 99:6080–6084
- Monforte AJ, Oliver M, Gonzalo MJ, Alvarez JM, Dolcet-Sanjuan R, Arús P (2004) Identification of quantitative trait loci involved in fruit quality traits in melon (*Cucumis melo* L.). *Theor Appl Genet* 108(4):750–758. doi:10.1007/s00122-003-1483-x
- Munger HM, Robinson RW (1991) Nomenclature of *Cucumis melo* L. *Cucurbit Genet Coop Rep* 14:43–44
- Nei M (1973) Analysis of gene diversity in subdivided populations. *Proc Natl Acad Sci USA* 70:3321–3323
- Nimmakayala P, Tomason YR, Jeong J, Vajja G, Levi A, Gibson P, Reddy UK (2009) Molecular diversity in the Ukrainian melon collection as revealed by AFLPs and microsatellites. *Plant Genet Resour* 7:127–134. doi:10.1017/S1479262108098481
- Nordborg M, Tavaré S (2002) Linkage disequilibrium: what history has to tell us. *Trends Genet* 18:83–90
- Ohashi J, Tokunaga K (2003) Power of genome-wide linkage disequilibrium testing by using microsatellite markers. *J Hum Genet* 48:487–491
- Pangalo KI (1958) Melons [Dyuni]. State publisher [Gosudarstvennoe izdatel'stvo]
- Paris M, Zalapa J, McCreight J, Staub J (2008) Genetic dissection of fruit quality components in melon (*Cucumis melo* L.) using a RIL population derived from exotic × elite US Western Shipping germplasm. *Mol Breeding* 22(3):405–419. doi:10.1007/s11032-008-9185-3
- Park SDE (2001) The Excel microsatellite toolkit. <http://animalgenomics.ucd.ie/sdepark/ms-toolkit/>
- Pitrat M (2008) Melon, vegetables I. In: Prohens J, Nuez F (eds) *Handbook of plant breeding*, vol 1. Springer, New York, pp 283–315. doi:10.1007/978-0-387-30443-4\_9
- Pritchard JK, Stephens M, Donnelly P (2000) Inference of population structure using multilocus genotype data. *Genetics* 155:945–959
- Pyzhenkov VI, Malinina MI (1994) Cucurbits (Cucumber, Melon). *Flora of Cultivated Plants XXI. Kolos, Moscow*, pp 200–288 (Russian)
- Remington DL, Thornsberry JM, Matsuoka Y, Wilson LM, Whitt SR, Doebley J, Kresovich S, Goodman MM, Buckler ES (2001) Structure of linkage disequilibrium and phenotypic associations in the maize genome. *Proc Natl Acad Sci USA* 98:11479–11484
- Risch N, Merikangas K (1996) The future of genetic studies of complex human diseases. *Science* 273:1516–1517
- Robinson RW, Decker-Walters DS (1997) Cucurbits. In: *Crop production science in horticulture*. CABI Publishing, New York
- Rousset F (2008) Genepop'007: a complete reimplementation of the Genepop software for Windows and Linux. *Mol Ecol Resour* 8:103–106
- Schneider S, Roessli D, Excoffier L (2000) Arlequin: a software for population genetics data analysis—user manual
- Sebastian PM, Schaefer H, Telford IRH, Renner SS (2010) Cucumber and melon have their wild progenitors in India, and the sister species of *Cucumis melo* L. is from Australia. *Proc Natl Acad Sci USA* 107(32):14269–14273
- Sidak Z (1967) Rectangular confidence region for the means of multivariate normal distributions. *J Am Stat Assoc* 62:626–633
- Silberstein L, Kovalski I, Huang R, Anagnostou K, Jahn MM, Perl-Treves R (1999) Molecular variation in melo (*Cucumis melo* L.) as revealed by RFLP and RAPD markers. *Sci Hortic* 79:101–111
- Slatkin M (1985) Gene flow in natural populations. *Annu Rev Ecol Syst* 16:393–430
- Staub J, Danin-Poleg Y, Fazio G, Horejsi T, Reis N, Katzir N (2000) Comparative analysis of cultivated melon groups (*Cucumis melo* L.) using random amplified polymorphic DNA and simple sequence repeat markers. *Euphytica* 115(3):225–241. doi:10.1023/a:1004054014174
- Stepansky A, Kovalski I, Perl-Treves R (1999) Intraspecific classification of melons (*Cucumis melo* L.) in view of their phenotypic and molecular variation. *Plant Syst Evol* 217:313–333
- Tanaka K, Nishitani A, Akashi Y, Sakata Y, Nishida H, Yoshino H, Kato K (2007) Molecular characterization of South and East Asian melon, *Cucumis melo* L., and the origin of Group Conomon var. *makuwa* and var. *conomon* revealed by RAPD analysis. *Euphytica* 153:233–247
- Tomason Y (2002) Selection of melon lines with female flower type and morphological markers to create heterotic F1 hybrids. PhD Dnepropetrovsk State Agrarian University
- Watterson GA (1978) Homozygosity test of neutrality. *Genetics* 88(2):405–417
- Weir BS, Cockerham CC (1984) Estimating F-statistics for the analysis of population structure. *Evolution* 38:1358–1370
- Xiao Y, Cai D, Yang W, Ye W, Younas M, Wu J, Liu K (2012) Genetic structure and linkage disequilibrium pattern of a rapeseed (*Brassica napus* L.) association mapping panel revealed by microsatellites. *Theor Appl Genet* 125(3):437–447. doi:10.1007/s00122-012-1843-5
- Yang X, Xu Y, Shah T, Li H, Han Z, Li J, Yan J (2011) Comparison of SSRs and SNPs in assessment of genetic relatedness in maize. *Genetica* 139:1045–1054. doi:10.1007/s10709-011-9606-9
- Yeh FC, Yang RC, Boyle T (1999) POPGENE Version 1.31. Microsoft Window-based freeware for population genetic analysis quick user guide
- Yu J, Buckler ES (2006) Genetic association mapping and genome organization of maize. *Curr Opin Biotechnol* 17:155–160
- Zalapa J, Staub J, McCreight J, Chung S, Cuevas H (2007) Detection of QTL for yield-related traits using recombinant inbred lines derived from exotic and elite US Western Shipping melon germplasm. *Theor Appl Genet* 114(7):1185–1201. doi:10.1007/s00122-007-0510-8
- Zhang J, Hao C, Ren Q, Chang X, Liu G, Jing R (2011) Association mapping of dynamic developmental plant height in common wheat. *Planta* 234:891–902
- Zhao K, Aranzana MJ, Kim S, Lister C (2007) An Arabidopsis example of association mapping in structured samples. *PLoS Genet* 3:71–82
- Zhu C, Gore M, Buckler ES, Yu J (2008) Status and prospects of association mapping in plants. *Plant Genome* 1:5–20